



OPEN

Mannan-binding lectin serine protease-2 (MASP-2) in human kidney and its relevance for proteolytic activation of the epithelial sodium channel

Rikke Zachar¹✉, Steffen Thiel², Søren Hansen³, Maiken Lumby Henriksen³, Mikkel-Ole Skjoedt⁴, Karsten Skjodt³, Zohra Hamzaei¹, Kirsten Madsen^{1,5}, Lars Lund⁶, Edith Hummler⁷, Per Svenningsen¹ & Boye Lagerbon Jensen^{1,6}

Proteolytic activation of the renal epithelial sodium channel (ENaC) is increased by aldosterone. The aldosterone-sensitive protease remains unidentified. In humans, elevated circulating aldosterone is associated with increased urinary extracellular vesicle (uEVs) excretion of mannan-binding lectin associated serine protease-2 (MASP-2). We hypothesized that MASP-2 is a physiologically relevant ENaC-activating protease. It was confirmed that MASP2 mRNA is abundantly present in liver but not in human and mouse kidneys. Aldosterone-stimulation of murine cortical collecting duct (mCCD) cells did not induce MASP-2 mRNA. In human kidney collecting duct, MASP-2 protein was detected in AQP2-negative/ATP6VB1-positive intercalated cells suggestive of MASP2 protein uptake. Plasma concentration of full-length MASP-2 and the short splice variant MAP19 were not changed in a cross-over intervention study in healthy humans with low (70 mmol/day) versus high (250 mmol/day) Na⁺ intake despite changes in aldosterone. The ratio of MAP19/MASP-2 in plasma was significantly increased with a high Na⁺ diet and the ratio correlated with changes in aldosterone and fractional Na⁺ excretion. MASP-2 was not detected in crude urine or in uEVs. MASP2 activated an amiloride-sensitive current when co-expressed with ENaC in *Xenopus* oocytes, but not when added to the bath solution. In monolayers of collecting duct M1 cells, MASP2 expression did not increase amiloride-sensitive current and in HEK293 cells, MASP-2 did not affect γ ENaC cleavage. MASP-2 is neither expressed nor co-localized and co-regulated with ENaC in the human kidney or in urine after low Na⁺ intake. MASP-2 does not mediate physiological ENaC cleavage in low salt/high aldosterone settings.

The epithelial Na⁺ channel (ENaC) in the kidney collecting duct principal cells plays an essential role in regulation of renal Na⁺ excretion and blood pressure. The Na⁺-retaining hormone aldosterone induces a shift in the molecular weight of the ENaC γ -subunit, consistent with post-translational proteolytic cleavage of its extracellular loop, leading to its activation^{1–4}. Proteolytic activation of ENaC in the apical membrane by cleavage of the extracellular loop contributes both to physiological, Na⁺-sensitive, and aberrant, pathophysiological, regulation of ENaC activity^{1,2,5}. Although the increased proteolytic processing of ENaC could be a consequence of increased plasma membrane localization, it is not known whether an aldosterone-sensitive “physiologica” protease is responsible for activation of ENaC.

Several proteases have been shown to activate ENaC in vitro; however, murine gene knockout studies show that the proteases prostasin, kallikrein and TMPRSS4 are dispensable for physiological proteolytic activation^{3,6–10}.

¹Department of Cardiovascular and Renal Research, Institute of Molecular Medicine, University of Southern Denmark, J.B. Winsløvsvej 21, 3, 5000 Odense, Denmark. ²Department of Biomedicine, Aarhus University, Aarhus, Denmark. ³Department of Cancer and Inflammation, Institute of Molecular Medicine, University of Southern Denmark, Odense, Denmark. ⁴Department of Clinical Immunology, Copenhagen University Hospital, Copenhagen, Denmark. ⁵Department of Pathology, Odense University Hospital, Odense, Denmark. ⁶Urology and Clinical Department, Odense University Hospital, Odense, Denmark. ⁷Department of Biomedical Sciences, University of Lausanne, Lausanne, Switzerland. ✉email: rzachar@health.sdu.dk

Urokinase, which is expressed along the nephron and present in urine, fails also to activate ENaC^{5,11}. Plasmin is present in minute amounts in urine from healthy individuals and not regulated by aldosterone and is therefore not a likely candidate for physiological regulation, and similar consideration applies for Cathepsin B¹² and factor VII activating protease (FSAP)¹³. Elevated circulating aldosterone levels, due either to salt-depletion or aldosterone infusion in patients with mild hypertension, increased the excretion of mannan-binding lectin associated serine protease 2 (MASP-2 (protein)/MASP2 (gene)) in urinary extracellular vesicles (EVs)¹⁴, which are nano-sized vesicles released from all nephron segments, containing proteins from their parental cell¹⁵. MASP-2 is necessary for activation of the lectin pathway of the complement system by forming complexes with the soluble pattern recognition molecules (PRMs) mannan-binding lectin (MBL), ficolins (H-, L- and M-ficolins) or collectins (Collectin L1 and K1). MASP-2 is activated when the PRMs bind to carbohydrate residues on microorganisms or “stressed” epithelial cells, leading to potential complement-system-mediated elimination or dysfunction of the target cell¹⁶.

The urinary excretion of MASP-2 in normal urine samples and its association with uEVs from healthy control persons and essential hypertensive patients was independently confirmed by proteomic analyses^{17,18}. Although the identification by mass spectrometry at the protein level confirms MASP-2 protein in urine, its expression in the kidney is controversial. MASP2 mRNA appears to be almost exclusively expressed in the liver and the MASP-2 protein circulates in plasma^{19,20}. The molecular weight of the full-length zymogen form of MASP-2 (~75 kDa) precludes any significant glomerular filtration in healthy persons. On the other hand, MASP-2 protein has been detected in the human kidney by immunohistochemistry²⁰, indicating either local expression or basolateral uptake and apical release leading to urinary excretion. Importantly, the previous studies do not take into account that there is also a splice variant produced from the MASP2 gene, i.e. MAp19, which lacks the catalytic domain but is still able to bind to MBL and ficolin²⁰. MAp19 is predominantly expressed in the liver, but the kidneys and thyroid gland have also been detected as sites of expression²⁰. While MAp19 has been suggested as a competitive inhibitor of complement activation by MASP-2²¹, this does not appear to be physiologically relevant since the affinity for MAp19 binding to PRMs is much lower than for MASP-2²⁰. MAp19 has also been suggested to act as an inhibitor of calcium oxalate kidney stone formation in human urine²², and a recent study showed an association between baseline serum MAp19 concentration and the incidence of microalbuminuria in a study cohort of 270 persons with newly diagnosed type 1 diabetes in an 18-year follow up study²³. Yet, the role of MAp19 in the kidney remains unknown. The present study focused on the observations of increased MASP-2 in human urine by low salt intake¹⁴ and present a comprehensive characterization of MASP2 in plasma, urine and tissue in humans.

Specifically, the aims of the present study were: (1) to map MASP-2 protein in human kidney tissue, (2) to study its possible regulation in plasma, urine and tissue by low salt/elevated aldosterone in healthy humans and (3) to elucidate its potential to activate ENaC proteolytically. Experiments were designed to test the hypotheses that MASP2 is co-expressed with ENaC in the human kidney collecting duct and its expression is stimulated by aldosterone, and that MASP-2 cleaves and activates γ -ENaC. The hypotheses were tested by application of monoclonal anti-human MASP-2 antibodies to tissue sections in immunohistochemistry and to tissue homogenates, urine and plasma for immunoblotting combined with specific and sensitive ELISAs directed against MASP-2 and MAp19. Moreover, *in vitro* experiments were done in heterologous expression systems with ENaC to examine effects on ENaC-mediated current by MASP-2 overexpression and MASP-2 addition.

Methods

Human kidney and liver tissue. Human kidney tissue was obtained from the Department of Urology, Odense University Hospital from patients undergoing nephrectomy due to renal cancer. As a routine, the patients had fasted 6 h before the operation, and all medicine was discontinued on the day of surgery. The tissue was taken from a non-tumorous part of the kidney and separated into the cortex, outer- and inner medulla 45–60 min after removing the kidney and frozen in liquid nitrogen or fixed in formalin. All patients gave informed written consent; the Ethics Committee of the Region of Southern Denmark (S-20140159) approved the study and the National Data Protection Authority (2012-58-0018) approved the study. The study was conducted according to the declaration of Helsinki. Pools of $n=4$ patients were made from the cortex, inner and outer medulla, respectively. Kidney tissue from patients receiving diuretics ($n=3$) with predicted high levels of aldosterone were compared to controls receiving no medicine ($n=4$). Patient information is shown in Table 1. Anonymized human liver tissue was obtained from patients undergoing liver resection at the Department of Abdominal Surgery, Odense University Hospital. Pools contained samples from 4 patients. The tissue was frozen in liquid nitrogen 45–60 min after removal, homogenized in lysis buffer ((20 mM Tris-HCl, 150 mM NaCl, 20 mM NaF, 10 mM Na₄P₂O₇, 1% Triton X-100) (Merck) with protease inhibitor (CComplete, Roche, Merck)) and frozen at -80 °C. Protein concentration was measured with the DC protein assay (BioRad).

Salt intervention samples. Plasma, urine, and uEV samples from a previous study²⁴ were included. The included test subjects ($n=10$) were given high (250 mmol/day) or low (70 mmol/day) Na⁺ diet for 5 days followed by sample collection and measurement before cross over to the opposite Na⁺ diet. The study was approved by the Ethics Committee of the Region of Southern Denmark (S-20150208), performed in accordance with the Helsinki Declaration, and registered at ClinicalTrials.gov as NCT02823613. All participants gave written informed consent, and the National Data Protection Authority (16/15900) approved the study. Further description of inclusion- and exclusion criteria is outlined in the original paper²⁴.

Urinary extracellular vesicles. Urine from healthy control persons was added protease-inhibitor (Complete, Roche, Merck) and frozen at -80 °C. The urine was thawed and vortexed for 1 min. Initial centrifuga-

Patient category	Patient id (western blot lane number)	Medicine	Gender (male/female)	Age (years)	Blood pressure (mmHg)
Control (no medicine)	1		F	41	139/69
	2		M	45	136/91
	3		M	72	155/83
	4		F	69	150/78
Diuretics (predicted high aldosterone)	1	Thiazide	F	66	190/90
	2	Loop diuretic	F	56	140/90
	3	Thiazide, alpha-blocker, β -blocker, Ca^{2+} antagonist	M	80	115/56

Table 1. Patient information—human kidney tissue. Patient information regarding medicine (pharmacological group), gender, age, and blood pressure from whom kidney tissue was obtained. *M* male, *F* female.

tion was performed at 3000g, 4 °C for 30 min, and the supernatant was centrifuged at 220,000g, at 4 °C for 100 min. The obtained pellet was re-suspended in imidazole buffer (250 mM sucrose, 25 mM imidazole, 1 mM EDTA- Na_2 ; Merck) with protease inhibitor (C0mplete, Roche, Merck), pH = 7.2) in a volume corresponding to 1/1000th of the original volume and frozen at -80 °C. All patients gave informed written consent, and the Ethics Committee of the Region of Southern Denmark (S-20150208) approved the study, and the project was reported to the National Data Protection Authority (18/31930). When performing western blotting, the uEVs were loaded according to the creatinine concentration of the original urine sample (2.7 $\mu\text{g}/\text{well}$).

Gel electrophoresis and immunoblotting. The samples were mixed with LDS Sample buffer (NuPAGE, Thermo Fisher Scientific) and reducing agent (NuPAGE) and denatured at 95 °C for 5 min before loading on a 4–12% Bis-Tris gel (NuPAGE). Electrophoresis was performed at 200 V using MOPS-buffer (NuPAGE) and precision Plus Protein Dual Color Standards (Bio-Rad). The proteins were transferred to 0.45 μm Immobilon-P PVDF membranes (Millipore) at 35 V for 1 h in transfer buffer (NuPAGE) with 10% ethanol (Merck). The membrane was blocked with 5% skimmed milk (Merck) in TBST (20 mM Tris-Base, 137 mM NaCl, 0.05% Tween-20 (Merck), pH = 7.6) for 1 h and incubated with primary antibody at 4 °C overnight. An *in-house* mouse monoclonal antibody targeting the SP-domain of MASP-2 (Fig. 2A,B) was used. It was raised against a human MASP-2 peptide aa575-584 LTQRGFLAR coupled to diphtheria toxoid and used for immunization, subsequently cloned and selected essentially as previously described²⁵. In addition, a monoclonal antibody, targeting the A-chain (clone 1.3B7), previously validated²⁶, was also used as primary antibody (Fig. 2A,B). For comparison and validation, a commercial mouse monoclonal antibody targeting the SP-domain of MASP-2 (OriGene Technologies, CAT#: TA812533S) was also applied (Fig. 2A,B). To detect ENaC cleavage in HEK293 cells, rabbit anti-rat gamma ENaC (Stress Marq, SPC-405) diluted 1:1000 was used. Anti- β -actin (Abcam, 8227) was used as a loading control. The membrane was washed with TBST and incubated with HRP-conjugated goat-anti mouse-IgG (0447, Dako), goat-anti rabbit-IgG (P0448, Dako), or rabbit-anti goat-IgG (P0449, Dako) antibody for 1 h. After a subsequent washing step with TBST, ECL (Amersham Bioscience) was applied, and signal developed using ChemiDo XRS + System with Image Lab Software (Bio-Rad). Densitometric analyses were done using Image lab Gel Doc (Bio-Rad). Uncropped original blots are presented in supplementary Fig. S2 and S4.

Immunohistochemistry and immunofluorescence. Kidney and liver samples were fixed in 4% paraformaldehyde (Merck) and embedded in paraffin. Blocks were cut in 1–4 μm sections, dewaxed, and rehydrated through a series of Tissue-Clear (Sakura ProHosp, Alphen an den Rijn, The Netherlands) and ethanol (99–70%) (Merck). Antigen retrieval was performed with TEG-buffer (10 mM TrisBase, 0.5 mM EGTA Tritriplex VI) (Merck) in a microwave oven for 20 min. Sections were washed in TBST (Merck) and blocked for 30 min in 3% Bovine Serum Albumin (BSA)/TBST (Merck), washed and blocked 10 min in hydrogen peroxide. Anti-MASP-2 (15-17-3) was applied undiluted/in culture supernatant overnight at 4 °C, washed, and incubated with HRP-conjugated goat-anti mouse-IgG (P0447; Dako) diluted 1:1000 for 1 h. Staining was visualized with 3,3'-diaminobenzidine (DAB)(Dako) and counterstained with Mayer's Hematoxylin (Merck). Images were taken with Olympus BX51 microscope with a DP26 camera and Cell Sens software (Olympus, Tokyo, Japan). Colocalization was investigated using anti-MASP-2, anti-AQP2 (collecting duct, principal cell marker, 1:200, 9882, Santa Cruz) and anti-ATP6V1B1 (collecting duct, intercalated cell marker, HPA031847, 1:50), respectively. AlexaFluor488 donkey-anti goat-IgG (Invitrogen) and AlexaFluor555 donkey-anti mouse-IgG (Invitrogen) were used as secondary antibodies.

Electrophysiological measurements in *Xenopus* oocytes. Purified cRNA was injected into stage V/VI oocytes isolated from *Xenopus laevis* (Noerdhoek, South Africa) as previously described²⁷. cRNA (0.25 ng), either coding for human or rat ENaC α , β and γ -ENaC were injected 24 h after harvesting, and oocytes were kept in MBS buffer (87.4 mM Na, 1 mM KCl, 86 mM NaHCO_3 , 2.4 mM HCO_3 , 0.8 mM MgSO_4 , pH = 7). Electrophysiological measurements were performed 48 h after injection. The oocytes were incubated in Frog Ringer solution (120 mM NaCl (or 50 mM as indicated), 2.5 mM KCl, 1.8 mM $\text{CaCl}_2 \cdot 2\text{H}_2\text{O}$, 10 mM HEPES buffer,

(Sigma-Aldrich) pH=7.2) with different concentrations of the MASP-2 protein for 20–30 min before electrophysiological measurements. Amiloride-sensitive Na current (I_{Na}) was recorded using a two-electrode voltage clamp, clamped at -80 V, defined as the difference between Na^+ current before and after amiloride. Trypsin was added to fully activate ENaC. Non-injected oocytes were included as negative controls in each experiment. Co-injection experiments were performed where cDNA encoding MASP-2 was subcloned into pSD5 expression vector and in vitro transcribed into cRNA. *Xenopus* oocytes were injected with different cRNA coding concentrations for MASP-2 together with human $\alpha\beta$ ENaC and incubated in MBS buffer for 24 h before electrophysiological measurements, as described above. Each figure represents a different batch of oocytes.

Electrophysiological measurement in M1 cells. M1 cells were cultured in Dulbecco's modified Eagle's medium (DMEM)/F12 1:1 (Invitrogen) supplemented with 10% fetal calve serum (FCS, Invitrogen) and pen-strep (Sigma) at 5% CO_2 at 37 °C. The media was changed every second day. Transfection with plasmid encoding MASP-2 was performed using Metafectene (Biontix, München, Germany). Non-transfected cells were included as controls. The cells were seeded onto permeable filter supports (pore size 0.4 μ m, surface area 4.67 cm^2 , Corning Costar), and transepithelial voltage (V_{te}) and resistance (R_{te}) were measured using an epithelial VoltOhmmeter (EVOM) (World Precision Instruments, Sarasota, FL, USA) on day 1–16 after transferring. On the last day of the experiments, 1 μ l of 50 μ M amiloride was added to each chamber and incubated for 2 min before measurements.

Measurement of ENaC cleavage in HEK cells. The cell line HEK293-ENaC was a kind gift from Prof. Olivier Staub, University of Lausanne. These cells are stably transfected with α ENaC, under the control of a glucocorticoid-inducible promoter, and β - and γ -ENaC expressed from a constitutive cytomegalovirus promoter²⁸.

Detection of MAP19 and MASP-2 in urine and plasma and purification of MASP-2 from serum. MAP19 and MASP-2 were measured in EDTA-plasma and urine with immunoassays described previously in detail^{20,29}. MASP-2 associated with PRMs was purified from serum from healthy control persons by incubating serum diluted in TBS containing 10 mM Ca^{2+} with a mixture of Sepharose bead coated with acetylated-HSA (binding H-ficolin and L-ficolin) and Mannose-TSK beads (binding MBL).

Mouse cortical collecting duct (mCCD) cells. mCCD cells (Clone 1, University of Lausanne) were cultured in growth media (DMEM/F12 1:1 (Invitrogen) supplemented with insulin (5 μ g/ml), apo-transferrin (5 μ g/ml), Na-selenate (60 nM), dexamethasone (50 nM), triiodothyronine (T3, 1 nM), penicillin (100 U/ml), streptomycin (130 μ g/ml), EGF (10 ng/ml) and 2% FBS (Thermo Fischer Scientific)) at 37 °C in 5% CO_2 . Cells were used between passages 23–30. Permeable filter supports (pore size 0.4 μ m, surface area 4.67 cm^2 ; Transwell, Corning Costar) were coated with Collagen Type I extracted from rat tail (Millipore) and polymerized for 30 min at room temperature by adding 250 μ l NH_3 aq (28%) in the empty compartments between the filters. The filters were incubated in growth media overnight at 37 °C in 5% CO_2 . mCCD cells were subcultured onto the filters and kept in growth media for 5 days, followed by culturing in the slightly modified growth media (DMEM/F12 1:1 with Insulin (5 μ g/ml), Na-selenate (60 nM), Dexamethasone (3 nM), T3 (1 nM), penicillin (100 U/ml) and streptomycin (130 μ g/ml) for 5 days. The media were changed every second day. Subsequently, the cells were incubated with experimental mCCD media (DMEM/F12 1:1 with penicillin (100 U/ml) and streptomycin (130 μ g/ml) with or without 300 nM aldosterone (Merck) for 24 h.

Polymerase chain reaction (PCR). RNA from mCCD cells was extracted using a RNeasy mini kit (Qiagen). cDNA was synthesized with PrimeScript RT reagent Kit (Takara) at 37 °C 15 min, 85 °C 5 s, and 4 °C. Quantitative real-time (qRT)-PCR was performed using PowerUp SYBR Green Master Mix (Thermo Fisher scientific) by incubating 2 min at 50 °C, 2 min at 95 °C; followed by 40 cycles of: 95 °C 15 s, 60 °C 1 min before being held at 4 °C. Primers targeting MASP2 (5'-ACCGCTGCGAGTATGACTTT-3', 5'-TGCATAGAAGGC CTCAAACC-3') were applied. The primers does not target the splice varian Map19. The data were analyzed by 7500 Fast Real-Time PCR systems with software v.2.04 (Applied Biosystems, Foster City, CA, USA). Human kidney and liver -tissue and mice tissue were RNA-extracted by phase separation using Trizol reagent (Merck). Turbo-DNAse free kit (Invitrogen) was applied, and cDNA was synthesized using the iScript cDNA Synthesis Kit (Bio-Rad). PCR amplification was performed with predesigned primer H_MASP2_3 (Sigma-Aldrich, Ref-Seq ID NM_006610) using PowerUp SYBR Green Master Mix (Thermo Fisher Scientific) at 95 °C for 3 min and 36 cycles of 95 °C 20 s, 60 °C 30 s, 72 °C 30 s, and 72 °C for 10 min before being held at 4 °C. The samples were separated on a 2% agarose gel with loading dye and a size marker (Sigma-Aldrich) at 125 V. H_2O , and samples without reverse transcriptase, GADPH, and β -actin were included as controls.

Statistics data access. Results were tested for normality using the Shapiro–Wilk normality test. If not normally distributed, log-transformation was performed, and data presented in a semi-logarithmic graph with geometric mean. Unpaired Student's t-test was used to test for differences. Correlations were investigated by linear regression. Graphs represent mean \pm SD. $P < 0.05$ were considered significant.

Results

MASP-2 protein is present in human kidneys. MASP-2 mRNA was not detected in human and murine kidney tissue while it was readily detected in human liver tissue (supplementary Fig. S1). To test if MASP-2 is present in the kidney at protein level. two different monoclonal anti-MASP-2 antibodies developed *in-house*

(15-17-3 and 13B7) and a commercial antibody (Origene TA812533S) were used to detect MASP-2 protein in human kidney and liver homogenates, in plasma and in urinary extracellular vesicles (uEVs) (Fig. 1A,B). Clone 15-17-3 targets the B-chain/serine protease (SP)-domain, whereas clone 13B.7 targets the A-chain of MASP-2, i.e., it reacts also with the alternative splice variant M_{Ap}19 (Fig. 1A,B). In the MASP-2 zymogen form, the A- and B-chains are connected via a peptide- and a disulfide bond (Fig. 1A,B). Once activated, it is only the disulfide bond that joins the A and B-chains. Thus, under reducing conditions, activated MASP-2 is predicted to migrate with separated A and B chains, as illustrated in Fig. 1B. In human kidney cortex tissue pool (n=4), the SP domain-directed antibody detected a significant band migrating at ≈ 70 kDa in both inner- and outer medulla and cortex (Fig. 1C). β -actin was used as loading control. Semi-quantification for each kidney specific tissue showed a linear correlation between concentration and western blot signal (supplementary Fig. S2A) A similar ≈ 70 kDa band was detected in a human liver tissue pool (n=4) (Fig. 1D). In plasma, the antibody reacted with a band that migrated at 75 kDa (Fig. 1E). Thus, full-length inactive MASP-2 that migrates with an apparent slightly lower molecular weight than in plasma is present in human kidney and liver tissue. By contrast, no full-length MASP-2 was detected in urinary extracellular vesicles (uEV) or experimentally concentrated crude urine (Fig. 1F). When using the antibody 137B, directed against the N-terminal domain, a ≈ 20 kDa band was detected in both urine and uEVs, corresponding to the alternative splice variant M_{Ap}19, while no signal for M_{Ap}19 was detected in human kidney cortex tissue (Fig. 1F). In urine and uEVs, the short isoform M_{Ap}19 is the dominant form. Because of the unexplained ~ 3 – 5 kDa difference in migration pattern between MASP-2 in plasma and fresh native tissue homogenates, specificity was further corroborated. Under non-reduced condition, the *in house* developed anti SP-domain antibody (15-17-3) resulted in a band in kidney cortex that migrated at 75 kDa and shifted to ~ 70 kDa under reduced conditions (Fig. 1G). A commercial antibody (OriGene #TA812533S) directed against the SP-domain confirmed the presence of a ≈ 75 kDa band under non-reduced conditions but did not seem to give clear signal in the reduced sample (Fig. 1G). In plasma, both antibodies recognized the zymogen form at 75 kDa (Fig. 1G). Other bands were exposed. Both anti-SP-antibodies recognized a band at ca 50 kDa and, at reducing conditions only, the beta-chain at ~ 25 kDa in tissue (Fig. 1G). We expect that the strong reactivity with bands at around 150–200 kDa in the non-reduced samples is due to reactivity with non-reduced IgG, i.e. the blot was developed with an anti-mouse IgG antibody, and some cross reactivity may be expected towards the human IgG on the blot. Both the commercial and the *in-house* antibody directed against the anti-SP domain detected a band ≈ 75 kDa, when a dilution series of pure human recombinant MASP-2 was present on the membrane (Fig. 1H).

MASP-2 immunoreactivity is present in intercalated cells in the human kidney collecting duct.

The antibody 15-17-3 directed against the SP-domain (Fig. 1A) revealed immune-positive signals from human liver sections, where the signal was associated with hepatocyte cytoplasm with a tendency to stronger labeling of zone III cells pericentrally (Fig. 2A,B). No signal was detected in the absence of a primary antibody (Fig. 2C). In kidney, an immune-positive staining was detected in both cortex, inner and outer medulla. Three different mAbs targeting the SP-domain showed similar results. The commercial monoclonal antibody targeting MASP-2 yielded similar staining pattern (Supplementary Fig. S3). Thus, labeling signal for MASP-2 was observed faintly in proximal convoluted tubules but not in glomeruli or in the vasculature (arteries and capillaries) (Fig. S3). MASP2 labeling was most prominent in the collecting ducts (Fig. 2D–F). More detailed analysis was performed in collecting ducts with special emphasis on principal cells, i.e. AQP2- positive cells, that express ENaC. In collecting ducts, the staining signal was localized mainly intracellularly, sparing the nucleus and with signal equally distributed at apical and basolateral sides (Fig. 2F). Confocal immunofluorescence detection confirmed MASP-2 localization in the collecting duct, where MASP-2 signal co-localized with the intercalated cell marker ATP6V1B1 (Fig. 2H,I). No co-localization with the principal cell-marker aquaporin-2 was detected (Fig. 2G). Thus, in the collecting ducts, MASP-2 is present in intercalated cells, and a direct intracellular interaction between ENaC and MASP2 is not likely under physiological conditions.

Effect of sodium intake/circulating aldosterone on MASP-2 concentration in urine and plasma.

Next, we tested the hypothesis that MASP-2 secretion is dependent on aldosterone concentration in humans under normal physiological settings. By ELISA, there was no difference in plasma concentration of MASP-2 (Fig. 3A, $p=0.5735$) or M_{Ap}19 (Fig. 3B, $p=0.1152$) in healthy adult males receiving high (250 mmol/day) or low (70 mmol/day) Na⁺ diet. A low Na⁺ diet decreased significantly the plasma ratio M_{Ap}19/MASP-2 (Fig. 3C, $p=0.0009$). The M_{Ap}19/MASP-2 ratio of the two isoforms produced from the MASP2 gene did not correlate with p-aldosterone concentration (Fig. 3D, $p=0.16$, $R^2=0.07$), but a significant correlation was detected between the delta values of p-aldosterone (Δ p-aldosterone = p-aldosterone-high Na⁺ minus p-aldosterone-low Na⁺) (Fig. 3E, $p=0.01$, $R^2=0.55$). AA positive correlation was detected between plasma M_{Ap}19/MASP-2 ratio and the fractional Na⁺-excretion (Fig. 3F, $p=0.03$, $R^2=0.16$). In urine, no difference in M_{Ap}19/creatinine concentration ratio between the two diets was detected (Fig. 3G, $p=0.82$). One test subject showed M_{Ap}19 below the detection limit in the urine samples from both high, low, and baseline samples, whereas another test person had M_{Ap}19 levels below detection range in the low Na⁺ period. The values below the detection range were not included in the statistical analysis. The ELISA assay did not detect any MASP-2 in crude or ex vivo experimentally concentrated urine. No correlation was detected between plasma aldosterone and MASP-2 concentrations ($p=0.13$), M_{Ap}19 ($p=0.28$) or urine M_{Ap}19 ($p=0.34$) or between mean arterial blood pressure and MASP-2 ($p=0.11$), plasma M_{Ap}19 ($p=0.14$) or urine M_{Ap}19 ($p=0.20$) (not shown). Furthermore, no correlation was detected between ratio M_{Ap}19/MASP-2 and uEV excretion of M_{Ap}19 ($p=0.10$, $R^2=0.10$) or M_{Ap}19 in the urine ($p=0.15$, $R^2=0.09$). There was a non-significant trend for more MASP-2 protein in kidney tissue from patients receiving diuretics (n=3) compared with controls receiving no medicine (n=4) (Fig. 3H, $p=0.1152$).

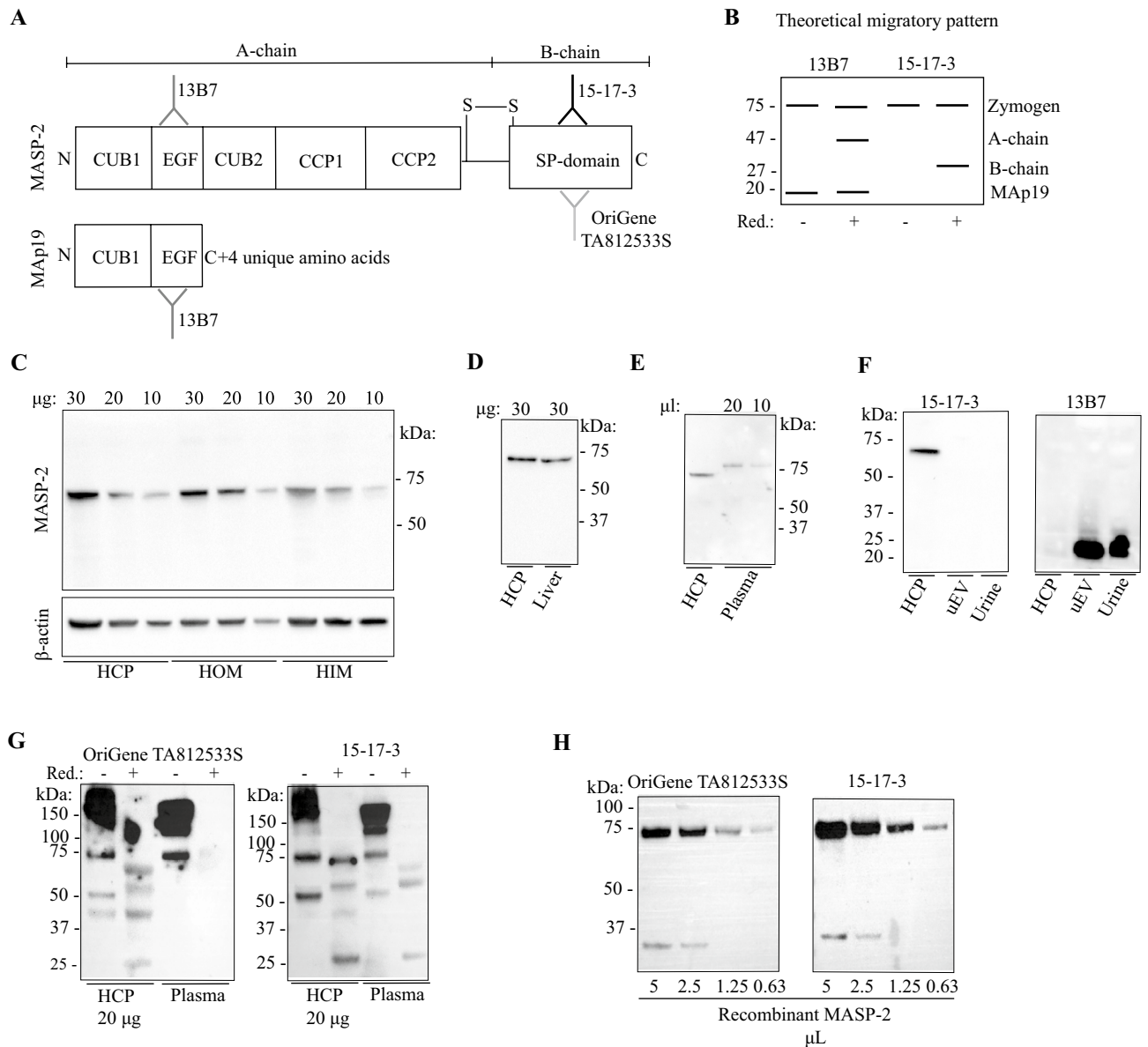


Figure 1. Detection of MASP-2 protein variants in liver, kidney and urine. **(A)** Three distinct murine monoclonal anti-human antibodies targeting MASP-2 were used, two reacting with epitopes within the SP-domain of MASP-2; an *in-house* (15-7-3) and a commercial (OriGene), the third (13B7) reacting with an epitope in the N-terminal domain. The six domains of intact MASP-2 are illustrated, including the two CUB-domains, the epidermal growth factor (EGF)-like domain, the two complement control repeats (CCPs) and the serine protease (SP) domain. The alternatively spliced short variant MASP19 also shown. N- and C-terminals are outlined. **(B)** Predicted cleavage products detected by the two antibodies. Under non-reduced conditions, the antibody targeting the A-chain (13B7) would detect bands at ≈ 75 kDa (MASP-2) and ≈ 20 kDa (MASP19), and the antibody targeting the B-chain (15-7-3) would detect at ≈ 75 kDa. Under reduced conditions, 13B7 is expected to detect the 47 kDa A-chain if MASP-2 is activated, whereas 15-7-3 antibody is expected to detect the 27 kDa variant (the SP-domain) (Fig. 2B, lane 3 + 4). **(C)** When using the anti-SP-antibody (15-17-3), a band ≈ 70 kDa was detected in human kidney homogenate in both human pools of kidney cortex (HCP, $n=4$), outer (HOM, $n=4$) and inner medulla (HIM, $n=4$) in reduced samples. **(D)** A similar band was detected in human liver homogenate, under reduced conditions, when using the anti-SP-antibody (15-17-3). HCP = human cortex pool ($n=4$). **(E)** In human plasma, the anti-SP-antibody (15-17-3) detected a band migrating at ≈ 75 kDa. **(F)** Full length MASP-2 was not detected with protein from urinary extracellular vesicles (uEV) or in experimentally concentrated urine when using the 15-17-3 antibody. When testing the antibody targeting the A-chain (13B7), no signal was detected in a kidney cortex pool (HCP, $n=4$). In contrast, the alternative splice variant MASP19 was detected in uEVs and concentrated urine. **(G)** Under non-reduced condition, a band likely representing intact MASP-2 at 75 kDa was apparent in kidney cortex (HCP) and plasma with the *in house* 15-17-3 antibody whereas the commercial monoclonal antibody (OriGene #TA812533S) directed against the SP domain confirmed the presence of a 75 kDa band in non-reducing lanes. Both antibodies detected a band migrating slightly faster, at ≈ 70 kDa, in a human kidney cortex pool (HCP) and plasma. **(H)** Both the commercial antibody (OriGene #TA812533S) and the *in-house* monoclonal antibody (15-17-3) detected a band ≈ 75 kDa, when recombinant MASP-2 was applied to the membrane under non-reduced conditions. Original uncropped blots are presented in Supplementary Fig. S2A–F.

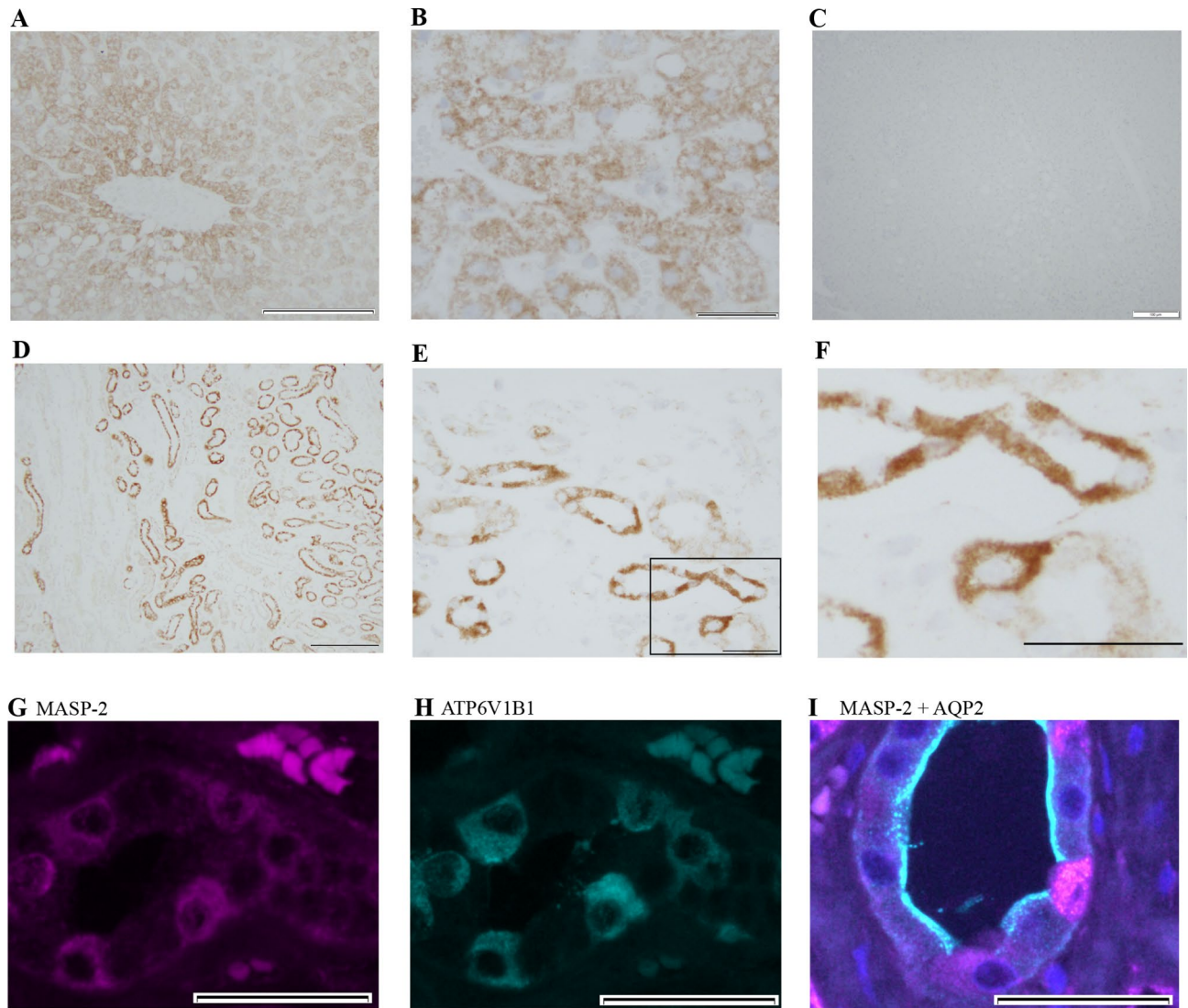


Figure 2. MASP-2 is localized in the intercalated cells of the collecting duct. (A,B) Using the antibody directed against the SP-domain of MASP-2 (15-17-3), immunohistochemical experiments revealed a positive signal in human liver sections that was associated with hepatocytes. (C) Negative control. (D–F) In human kidney sections, immunohistochemical signal from MASP-2 was detected in distinct tubular segments both in cortex and in medulla which were not proximal tubules. Along labeled segments, certain subsets of cells were not labeled (E,F). (G,H) MASP-2 co-localized with the intercalated cell marker ATP6V1B1. (I) MASP-2 did not co-localize with principal cell marker aquaporin-2 (AQP-2 turquoise, MASP-2 magenta, DAPI/nucleus = blue).

Effect of salt intake/plasma aldosterone on MASP-2 protein abundance in uEVs. To test for MASP-2-association with apical epithelial membranes along the tubular system, urine microvesicles were isolated and analyzed. Only MASP-2 and not full-length MASP-2 was detected in uEVs (Fig. 4A,B). No significant relation with plasma aldosterone concentration was detected in baseline samples between individuals when ranging according to measured plasma aldosterone (Fig. 4B). In paired samples, no difference in MASP-2 was detected between high and low dietary Na^+ intakes (Fig. 4C).

Co-expression of MASP-2 activates ENaC in vitro in *Xenopus* oocytes, but not in a stable cell line and no difference in ENaC cleavage products is detected. To investigate if MASP-2 is able to activate ENaC, we used *Xenopus* oocytes ENaC and MASP2 cRNA co-injected into *Xenopus* oocytes showed an increased amiloride-sensitive Na^+ current at 8 ng and 12 ng of MASP-2 cRNA (Fig. 5A, $p=0.003$). In contrast, incubating ENaC-cRNA injected oocytes with different concentrations of active MASP-2, no difference in amiloride-sensitive current was detected (Fig. 5B), neither when incubating with the associated pattern recognition molecule collectin CL-LK that forms complex with MASP-2 (Fig. 5C), nor when lowering the Na^+ concentration of the buffer (Fig. 5D). To validate the above results another in-vitro experiment was performed, using monolayers of collecting duct normal or MASP2 stable transfected M1 cells cultured on filters. Subsequent western blotting was performed to assure transfection and only cells transfected with MASP-2 gave a signal

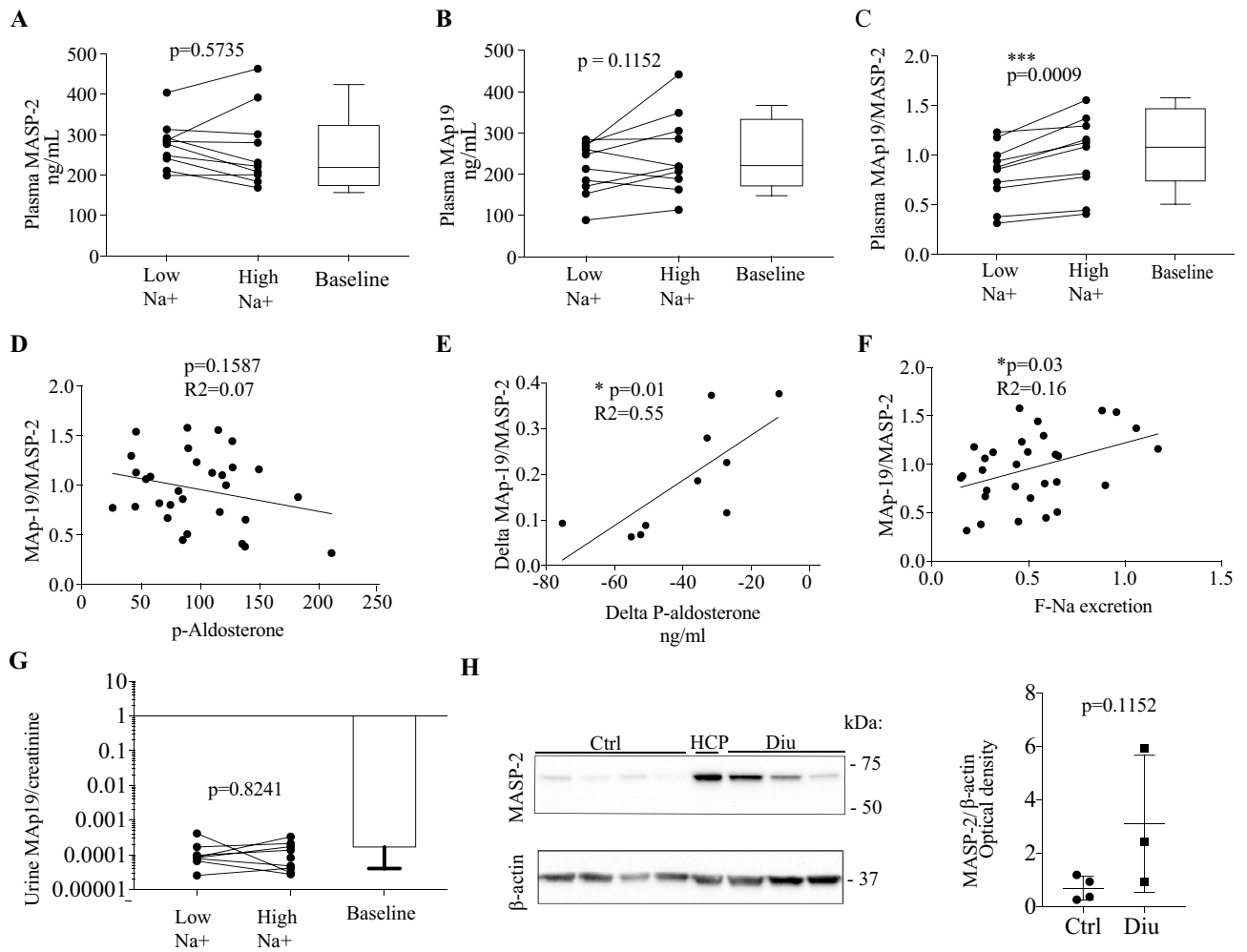


Figure 3. Changes in plasma concentration of MASP-2 and MASP-2 in response to Na⁺ intake. (**A,B**) In a cohort of healthy young men (n = 10) ingesting a diet with high (250 mmol/day) and low (70 mmol/day) Na⁺ content for five days, no difference was detected in plasma concentrations of MASP-2 and MASP-19 in response to Na⁺ intake. Samples obtained on habitual diet were analyzed to allow comparison and increased power in correlation analysis (indicated as baseline). (**C**) The MASP-19/MASP-2 ratio was significantly increased in conditions with high Na⁺ intake (p = 0.0009). (**D,E**) The ratio did not correlate with p-aldosterone (p = 0.16, R² = 0.07), but the delta values of p-aldosterone in the individuals correlated significantly with the delta values of ratio MASP-19/MASP-2 (p = 0.01, R² = 0.55). (**F**) Ratio MASP-19/MASP-2 correlated significantly with the fractional Na⁺ excretion (p = 0.03, R² = 0.16). (**G**) No difference in urine MASP-19/creatinine concentration ratio was detected with different Na⁺ intake (p = 0.82). Intact MASP-2 was not detected in the urine. (**H**) In kidney cortex homogenate from patients receiving diuretics (Diu) before nephrectomy and therefore with predicted higher plasma aldosterone concentration than in patients not receiving medicine (Ctrl), no significant difference in MASP-2 protein abundance was detected. Original uncropped blots are presented in Supplementary Fig. S2G. HCP = human kidney cortex pool, n = 4. p = plasma.

(supplementary Fig. S4A). No differences in amiloride-sensitive current were detected between cells transfected with MASP-2, compared to non-transfected cells when performing EVOM measurements (Fig. 6A). Amiloride was added the last day of experiment (day 16). No difference between the MASP-2 transfected cells and control cells was detected in voltage, current or resistance at any point of the experiment (supplementary Fig. S4B–D). To assess MASP2-induced γENaC cleavage, we used HEK293-cells with constitutive β- and γ-ENaC subunits expression and dexamethasone-inducible α-subunit expression. In these cells, ENaC is only surface localized in the presence of dexamethasone²⁸, and consistent with this, no γENaC cleavage was detected without dexamethasone (Fig. 6B). Incubation with soluble MASP2 protein did not affect ENaC cleavage compared to control in dexamethasone-treated cells (Fig. 6B).

Discussion

The present set of data show the presence of MASP-2 protein in human kidney collecting duct intercalated cells despite undetectable kidney MASP2 mRNA expression. MASP-2 can activate ENaC *in vitro* in *Xenopus* oocytes, while stable expression of MASP-2 in M-1 collecting ducts cells did not affect amiloride-sensitive transepithelial

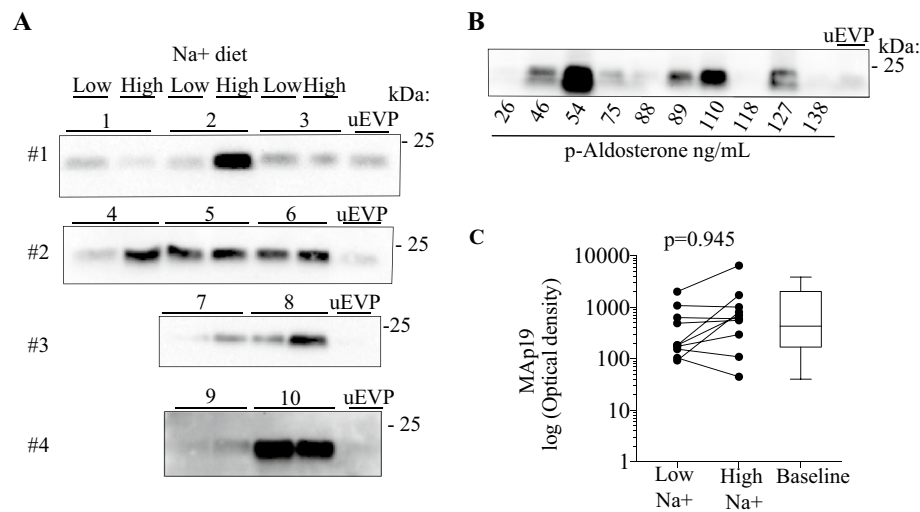


Figure 4. Effect of Na⁺ intake on MAP19 in urine extracellular vesicles. (A) In a cohort of healthy young men receiving high (250 mmol/day) and low (70 mmol/day) Na⁺ diet, MAP19 was detected in all uEVs. Original uncropped blots are presented in Supplementary Fig. S1H. (B) No clear correlation between abundance of uEV-associated MAP19 protein and plasma aldosterone concentration was observed when samples were subjected to SDS-PAGE and immunoblotting according to plasma aldosterone concentration. Original uncropped blots are presented in Supplementary Fig. S1I. (C) There was no significant intra individual difference of uEV-associated MAP19 protein abundance between high and low Na⁺ intake ($p=0.09$). The signal obtained with western blotting was normalized to the signal obtained from a pool of uEV (uEVP, $n=10$) to allow comparison between blots.

current, and no difference in ENaC-cleavage is revealed. In healthy young male adults, there were no changes in MASP-2 in plasma or urine that related to changes in sodium intake and aldosterone plasma concentration. There was an increased MAP19/MASP-2 ratio in plasma with high Na⁺-diet suggesting altered regulation of mRNA splicing. Taken together, MASP-2 is not likely to exert aldosterone-driven, luminal, physiological activation of ENaC by proteolytic cleavage of the γ -subunit.

In the present study, we showed that MASP-2 can activate ENaC in vitro when co-expressed in *Xenopus* oocytes, but not in MASP2 transfected M1 cells. On the other hand, soluble MASP2 did not activate ENaC in oocyte or cause γ ENaC cleavage in ENaC expressing HEK293. The reason for this difference is not known, but together this indicates that the role of MASP-2 in the kidney is less likely to involve ENaC regulation. In line with this, several other proteases have been shown to activate ENaC in vitro, including prostaticin^{4,9,30,31}, tissue-kallikrein³², plasma-kallikrein⁸ and TMPRSS4^{9,33}. However, when tested in vivo, typically by gene targeting of the proteases, no phenotypes were detected^{7,8,32}.

Since the surface binding of circulating MASPs requires specific interaction partners, we speculated that collectin CL-LK could be the link between ENaC and MASP-2 since it binds to mannose and L-fucose-rich structures and ENaC is known to be highly glycosylated when expressed on the surface³⁴. CL-LK is a soluble C-type lectin produced by several non-immune cells, including epithelial cells of the renal tract³⁵. However, activation was not observed when co-incubating soluble MASP-2 alone or in complex with collectin CL-LK, which is known to avidly form complex with MASP-2 and activate the complement system. CL-K1 binding activity is also strongly and positively modulated by low concentrations of Na⁺³⁶, but no difference was detected by lowering Na⁺ concentration.

Previous studies showed that MASP2 mRNA was almost exclusively expressed in the liver^{19,20,37}, which was confirmed in the present study, where no mRNA expression of MASP2 was detected in neither mice or humans. It is puzzling how MASP-2 protein enters the tubular epithelium. One study suggests that MASP-2 is filtered across the glomerular barrier despite its size³⁸; however, MASP-2 was not detected in urine or uEVs (MAP19 only). The finding of intact MASP-2 protein in the kidney is consistent with two previous studies showing diffuse but strong immunopositive signal in the kidney^{20,39}. The MASP-2 detected in kidney by western blotting is around 5 kDa below the MASP-2 detected in plasma. The molecular weight in kidney was confirmed using two independent monoclonal antibodies. We speculate that the difference in migration could be due to the active form of purified MASP-2 migrates slower on western blotting compared to the zymogen, which has previously been the case for the comparable MASP-1⁴⁰. In other words, it is the zymogen form of MASP-2 which appears to be present in the kidney tissue. In the present study, MASP-2 immunoreactivity was associated with the intercalated cells in the collecting duct and not in ENaC expressing AQP2-positive principal cells. Thus, a direct intracellular interaction between ENaC and MASP2 is not likely under physiological conditions. Previous studies have suggested that the intercalated cells play a role in the innate immune system⁴¹; however, the role of MASP-2 in intercalated cells is unknown. The mechanism for selective accumulation of zymogen MASP-2 in intercalated cells is not clear.

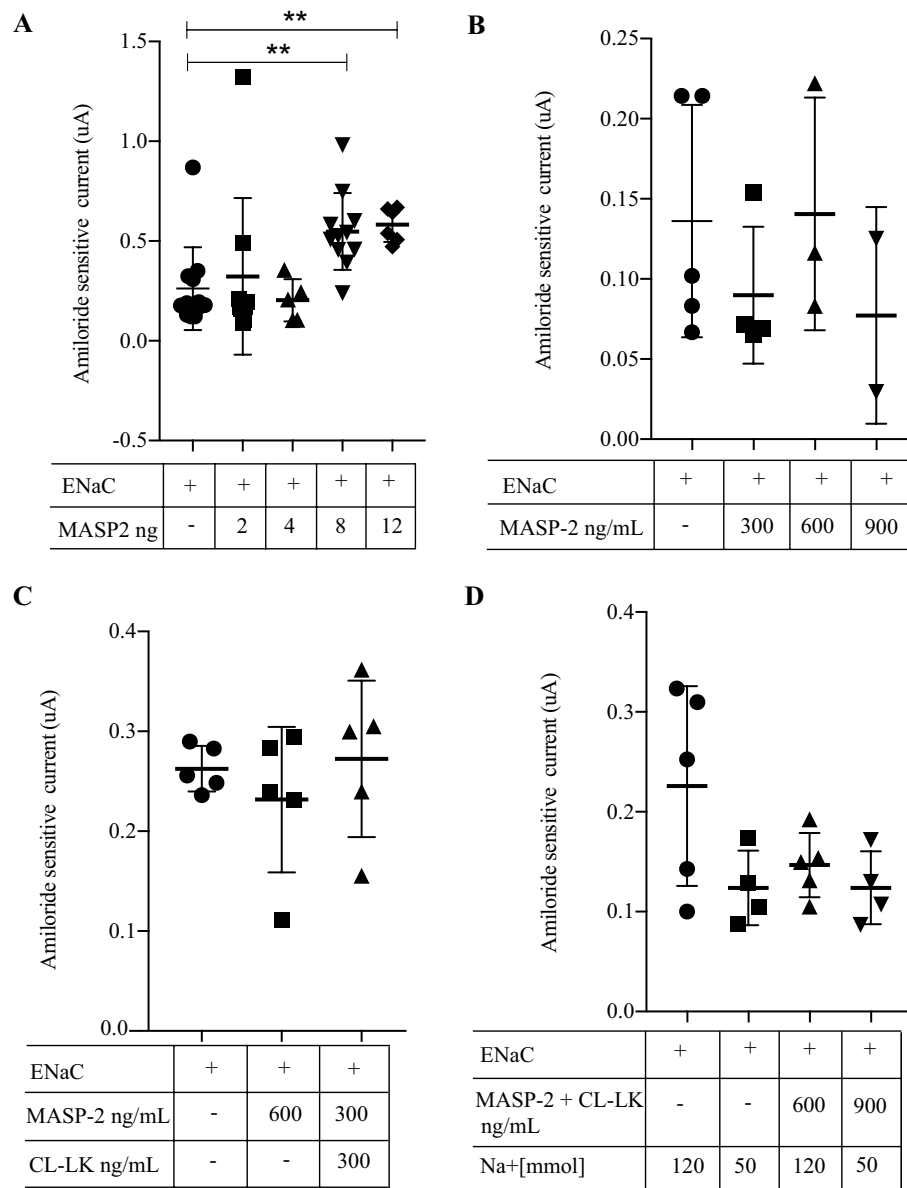


Figure 5. Effect of co-expression of MASP-2 and ENaC on current in *Xenopus* oocytes. (A) When co-injecting cRNAs for $\alpha\beta\gamma$ ENaC and MASP2, an increased amiloride-sensitive current was detected with a concentration of 8 and 12 ng MASP2. (B–D) In *Xenopus* oocytes injected with cRNAs encoding $\alpha\beta\gamma$ ENaC, no increased amiloride-sensitive current was detected when applying MASP-2 in the buffer, neither when adding the pattern recognition molecule collectin CL-LK (heteromer of collectin liver 1 and kidney 1), known to interact with MASP-2 (C), nor when decreasing the Na^+ concentration of the buffer (D).

Another interesting finding was that full length MASP-2 was not detected in urine and uEVs in seemingly contrast to previous studies^{14,18}. Since the referred studies utilized mass spectrometry-based proteome analysis of urine, we speculate that the detected MASP-2 in these studies based on peptide patterns was the short variant MAP19. The consistent detection of MAP19 in both uEVs and urine by redundant immunoblotting and ELISA further supports this interpretation. With a molecular size below 25 kDa a fraction in plasma would be filtered across the glomerular barrier. The previous study that reported significant regulation of MASP-2 by aldosterone¹⁴ did not reveal the peptide sequence used. When looking at the study by Damkjær et al., the peptide sequences used target MASP-2 at amino acids 21–56, meaning that it is likely the alternative splice variant MAP19¹⁸. Nevertheless, a study using activity-based protein profiling showed that MASP-2 was present in an active form in the urine¹⁷ and a recent study identified the individual proteases in urine from healthy and nephrotic humans and found MASP-2 to be one of the most abundant proteases in urine from healthy humans⁴².

We did not detect regulation of MASP-2 concentration by aldosterone. The plasma ratio of MAP19/MASP-2 was significantly decreased with low Na^+ intake, which could indicate that the MASP-2 splice variant's transcription is favored towards MAP19 in this condition. The plasma MAP19/MASP-2 ratio correlated significantly

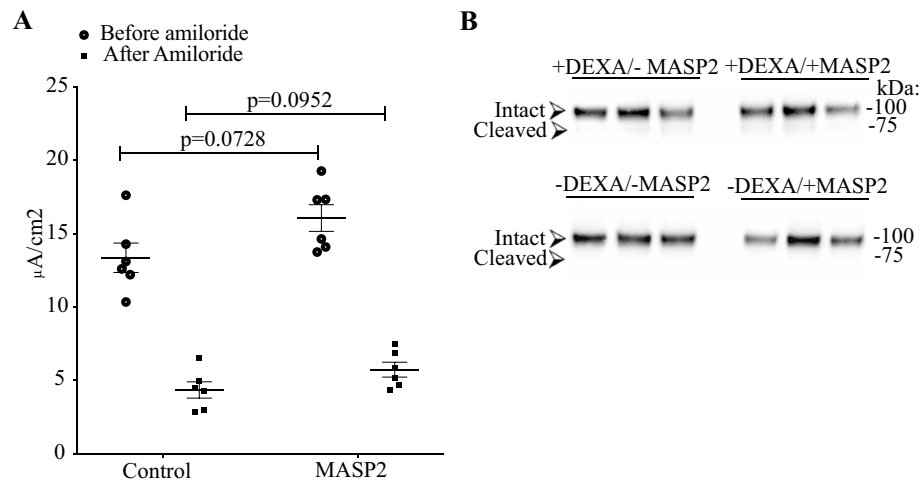


Figure 6. Transepithelial current responses in M1 cells transfected with MASP2. **(A)** No difference in Amiloride-sensitive current was detected between MASP-2 transfected and non-transfected M1 cells ($n=6$ experiments for each condition). The time course of transepithelial voltage, resistance or current for M1 cells transfected with MASP-2 and controls are shown in supplementary Fig. S4. **(B)** HEK293-cells with heterologous ENaC expression showed no difference in γ ENaC cleavage when subjected to MASP2. These cells constitutively express β - and γ -ENaC subunits, while the α -subunit is induced by dexamethasone (indicated as + DEXA). ENaC is, therefore, only surface localized in the presence of dexamethasone, and consistent with this, no γ ENaC cleavage was detected without dexamethasone. The predicted size of non-cleaved/intact and cleaved γ ENaC is indicated. Original uncropped blots are presented in Supplementary Fig. S2K.

with change in plasma aldosterone concentration, which is compatible with a causal relation. We speculate that aldosterone could regulate the transepithelial transport of MASP-2 and/or MAP19, as seen with other proteins like albumin⁴³. A previous study found no correlation between plasma MAP19 and urine excretion of MAP19, indicating that glomerular filtration couldn't fully account for urine MAP19²⁰. The lack of significant difference in the kidney tissue from patients receiving diuretics could be due to the small number of included patients and the use of medication which changes aldosterone (ACEi, AT1 blockers).

The physiological function of MASP-2 in the kidney is not clarified. MASP-2 has an established role in innate immunity and in certain pathophysiological conditions, it may promote kidney injury. Thus, absence of MASP-2 is protective in a transplant model of renal ischemia–reperfusion injury in mice⁴⁴. The absence of MASP-2 is also protective in protein overload nephropathy⁴⁵. MASP-2 contributes to IgA nephropathy, and an antibody against MASP-2 to treat IgA nephropathy (OMS721, Omeros, Seattle, WA, USA) is currently under investigation, where the phase-2 trial showed reduced proteinuria in IgA nephropathy by 50–90% and stabilized or increased glomerular filtration rates when treating with the antibody (Clinical Trial ID: NCT02682407)⁴⁶.

In conclusion, full-length catalytically active MASP-2 can activate ENaC current in vitro when co-expressed in some experimental settings but does not appear to be co-expressed or co-localized with ENaC in the principal cells in human, is not present in intact form in urine and does not lead to ENaC cleavage ex vivo and is not regulated by aldosterone. Together, this indicates that MASP-2 is less likely to mediate physiological, proteolytic regulation of ENaC. The short MASP-2 isoform MAb19 is present in soluble and membrane bound form in urine and the ratio of MAP19 and MASP-2 changed with aldosterone. Its significance remains to be determined.

Data availability

The datasets generated and/or analysed during the current study are available in the figshare repository, <https://doi.org/10.6084/m9.figshare.19719208>.

Received: 23 April 2022; Accepted: 9 September 2022

Published online: 24 September 2022

References

- Masilamani, S., Kim, G. H., Mitchell, C., Wade, J. B. & Knepper, M. A. Aldosterone-mediated regulation of ENaC alpha, beta and gamma subunit proteins in rat kidney. *J. Clin. Investig.* **104**, R19–R23 (1999).
- Uchimura, K. *et al.* In vivo contribution of serine proteases to the proteolytic activation of gammaENaC in aldosterone-infused rats. *Am. J. Physiol. Renal Physiol.* **303**, F939–943. <https://doi.org/10.1152/ajprenal.00705.2011> (2012).
- Vallet, V., Chraïbi, A., Gaeggeler, H., Horisberger, J. & Rossier, B. C. An epithelial serine protease activates the amiloride-sensitive sodium channel. *Nature* **389**, 607–610 (1997).
- Vuagniaux, G. *et al.* Activation of the amiloride-sensitive epithelial sodium channel by the serine protease mCAP1 expressed in a mouse cortical collecting duct cell line. *J. Am. Soc. Nephrol.* **11**, 828–834 (2000).
- Svenningsen, P. *et al.* Plasmin in nephrotic urine activates the epithelial sodium channel. *J. Am. Soc. Nephrol.* **20**, 299–310. <https://doi.org/10.1681/ASN.2008040364> (2009).
- Colman, R. W. Activation of plasminogen by human plasma kallikrein. *Biochem. Biophys. Res. Commun.* **35**, 273–279 (1969).

7. Keppner, A. *et al.* Epithelial sodium channel-mediated sodium transport is not dependent on the membrane-bound serine protease CAP2/Tmprss4. *PLoS ONE* **10**, e0135224. <https://doi.org/10.1371/journal.pone.0135224> (2015).
8. Haerteis, S. *et al.* Plasma kallikrein activates the epithelial sodium channel in vitro but is not essential for volume retention in nephrotic mice. *Acta Physiol.* <https://doi.org/10.1111/apha.13060> (2018).
9. Vuagniaux, G., Vallet, V., Jaeger, N. F., Hummler, E. & Rossier, B. C. Synergistic activation of ENaC by three membrane-bound channel-activating serine proteases (mCAP1, mCAP2, and mCAP3) and serum- and glucocorticoid-regulated kinase (Sgk1) in *Xenopus* oocytes. *J. Gen. Physiol.* **120**, 191–201. <https://doi.org/10.1085/jgp.20028598> (2002).
10. Ehret, E. *et al.* Kidney-specific CAP1/Prss8-deficient mice maintain ENaC-mediated sodium balance through an aldosterone independent pathway. *Int. J. Mol. Sci.* **23**, 6745. <https://doi.org/10.3390/ijms23126745> (2022).
11. Bohnert, B. N. *et al.* Urokinase-type plasminogen activator (uPA) is not essential for epithelial sodium channel (ENaC)-mediated sodium retention in experimental nephrotic syndrome. *Acta Physiol.* <https://doi.org/10.1111/apha.13286> (2019).
12. Larionov, A. *et al.* Cathepsin B increases ENaC activity leading to hypertension early in nephrotic syndrome. *J. Cell Mol. Med.* **23**, 6543–6553. <https://doi.org/10.1111/jcmm.14387> (2019).
13. Artunc, F. *et al.* Proteolytic activation of the epithelial sodium channel (ENaC) by factor VII activating protease (FSAP) and its relevance for sodium retention in nephrotic mice. *Pflügers Arch. Eur. J. Physiol.* <https://doi.org/10.1007/s00424-021-02639-7> (2021).
14. Qi, Y. *et al.* Activation of the endogenous renin-angiotensin-aldosterone system or aldosterone administration increases urinary exosomal sodium channel excretion. *J. Am. Soc. Nephrol.* <https://doi.org/10.1681/ASN.2014111137> (2015).
15. Pisitkun, T., Shen, R. F. & Knepper, M. A. Identification and proteomic profiling of exosomes in human urine. *Proc. Natl. Acad. Sci. USA* **101**, 13368–13373. <https://doi.org/10.1073/pnas.0403453101> (2004).
16. Bajic, G., Degn, S. E., Thiel, S. & Andersen, G. R. Complement activation, regulation, and molecular basis for complement-related diseases. *EMBO J.* **34**, 2735–2757. <https://doi.org/10.15252/embj.201591881> (2015).
17. Navarrete, M. *et al.* Proteomic characterization of serine hydrolase activity and composition in normal urine. *Clin. Proteomics* **10**, 17 (2013).
18. Damkjaer, M. *et al.* Selective renal vasoconstriction, exaggerated natriuresis and excretion rates of exosomal proteins in essential hypertension. *Acta Physiol.* **212**, 106–118. <https://doi.org/10.1111/apha.12345> (2014).
19. Seyfarth, J., Garred, P. & Madsen, H. O. Extra-hepatic transcription of the human mannose-binding lectin gene (mbl2) and the MBL-associated serine protease 1–3 genes. *Mol. Immunol.* **43**, 962–971. <https://doi.org/10.1016/j.molimm.2005.06.033> (2006).
20. Degn, S. E. *et al.* MASP19, the alternative splice product of the MASP2 gene. *J. Immunol. Methods* **373**, 89–101. <https://doi.org/10.1016/j.jim.2011.08.006> (2011).
21. Iwaki, D. *et al.* Small mannose-binding lectin-associated protein plays a regulatory role in the lectin complement pathway. *J. Immunol.* **177**, 8626 (2006).
22. Kang, I. *et al.* Mannan-binding lectin (MBL)-associated plasma protein present in human urine inhibits calcium oxalate crystal growth. *FEBS Lett.* **462**, 89–93 (1999).
23. Ostergaard, J. A. *et al.* Incident microalbuminuria and complement factor mannan-binding lectin-associated protein 19 in people with newly diagnosed type 1 diabetes. *Diabetes Metab. Res. Rev.* **33**, e2895. <https://doi.org/10.1002/dmrr.2895> (2017).
24. Zachar, R., Jensen, B. L. & Svenningsen, P. Dietary Na⁺ intake in healthy humans changes the urine extracellular vesicle prostasin abundance while the vesicle excretion rate, NCC, and ENaC are not altered. *Am. J. Physiol.-Renal Physiol.* **317**, F1612–F1622. <https://doi.org/10.1152/ajprenal.00258.2019> (2019).
25. Pilely, K. *et al.* A specific assay for quantification of human C4c by use of an anti-C4c monoclonal antibody. *J. Immunol. Methods* **405**, 87–96 (2014).
26. Thiel, S. *et al.* Interaction of C1q and Mannan-binding lectin (MBL) with C1r, C1s, MBL-associated serine proteases 1 and 2, and the MBL-associated protein MASP19. *J. Immunol.* **165**, 878–887. <https://doi.org/10.4049/jimmunol.165.2.878> (2000).
27. Geering, K., Theulaz, I., Verrey, F., Hauptle, M. T. & Rossier, B. C. A role for the beta-subunit in the expression of functional Na⁺-K-ATPase in *Xenopus* oocytes. *Am. J. Physiol.* **257**, C851–C858 (1989).
28. Ruffieux-Daidie, D. *et al.* Deubiquitylation regulates activation and proteolytic cleavage of ENaC. *J. Am. Soc. Nephrol.* **19**, 2170–2180. <https://doi.org/10.1681/ASN.2007101130> (2008).
29. Møller-Kristensen, M. *et al.* Levels of mannan-binding lectin-associated serine protease-2 in healthy individuals. *J. Immunol. Methods* **282**, 159–167. <https://doi.org/10.1016/j.jim.2003.08.012> (2003).
30. Adachi, M. *et al.* Activation of epithelial sodium channels by prostasin in *Xenopus* oocytes. *J. Am. Soc. Nephrol.* **12**, 1114–1121 (2001).
31. Narikiyo, T. *et al.* Regulation of prostasin by aldosterone in the kidney. *J. Clin. Investig.* **109**, 401–408. <https://doi.org/10.1172/jci0213229> (2002).
32. Picard, N. *et al.* Defective ENaC processing and function in tissue kallikrein-deficient mice. *J. Biol. Chem.* **283**, 4602–4611 (2008).
33. Passero, C. J. *et al.* TMPRSS4-dependent activation of the epithelial sodium channel requires cleavage of the gamma-subunit distal to the furin cleavage site. *Am. J. Physiol. Renal Physiol.* **302**, F1–8. <https://doi.org/10.1152/ajprenal.00330.2011> (2012).
34. Farrar, C. A. *et al.* Collectin-11 detects stress-induced L-fucose pattern to trigger renal epithelial injury. *J. Clin. Investig.* **126**, 1911–1925. <https://doi.org/10.1172/JCI83000> (2016).
35. Hansen, S. *et al.* Collectin 11 (CL-11, CL-K1) is a MASP-1/3-associated plasma collectin with microbial-binding activity. *J. Immunol.* **185**, 6096–6104. <https://doi.org/10.4049/jimmunol.1002185> (2010).
36. Henriksen, M. L. *et al.* Heteromeric complexes of native collectin kidney 1 and collectin liver 1 are found in the circulation with MASPs and activate the complement system. *J. Immunol.* **191**, 6117–6127. <https://doi.org/10.4049/jimmunol.1302121> (2013).
37. Stover, C. M., Thiel, S., Lynch, N. J. & Schwaeble, W. J. The rat and mouse homologues of MASP-2 and MASP19, components of the lectin activation pathway of complement. *J. Immunol.* **163**, 6848–6859 (1999).
38. Musante, L. *et al.* Characterization of plasma factors that alter the permeability to albumin within isolated glomeruli. *Proteomics Clin. Appl.* **2**, 197–205 (2002).
39. Huang, Y. *et al.* High expression of complement components in the kidneys of type 2 diabetic rats with diabetic nephropathy. *Front. Endocrinol.* **10**, 459. <https://doi.org/10.3389/fendo.2019.00459> (2019).
40. Oroszlán, G. *et al.* Extensive basal level activation of complement mannan-binding lectin-associated serine protease-3: Kinetic modeling of lectin pathway activation provides possible mechanism. *Front. Immunol.* **8**, 1821. <https://doi.org/10.3389/fimmu.2017.01821> (2017).
41. Breton, S. & Brown, D. Novel proinflammatory function of renal intercalated cells. *Ann. Nutr. Metab.* **72**(Suppl 2), 11–16. <https://doi.org/10.1159/000488303> (2018).
42. Wörn, M. *et al.* Proteasuria in nephrotic syndrome—quantification and proteomic profiling. *J. Proteomics* **230**, 103981. <https://doi.org/10.1016/j.jprot.2020.103981> (2021).
43. Jensen, T. B., Cheema, M. U., Szymiczek, A., Damkier, H. H. & Praetorius, J. Renal type a intercalated cells contain albumin in organelles with aldosterone-regulated abundance. *PLoS ONE* **10**, e0124902. <https://doi.org/10.1371/journal.pone.0124902> (2015).
44. Asgari, E. *et al.* Mannan-binding lectin-associated serine protease 2 is critical for the development of renal ischemia reperfusion injury and mediates tissue injury in the absence of complement C4. *FASEB J.* **28**, 3996–4003. <https://doi.org/10.1096/fj.13-246306> (2014).
45. Alghadban, S., Kenawy, H. I., Dudler, T., Schwaeble, W. J. & Brunskill, N. J. Absence of the lectin activation pathway of complement ameliorates proteinuria-induced renal injury. *Front. Immunol.* **10**, 2238. <https://doi.org/10.3389/fimmu.2019.02238> (2019).

46. Lafayette, R. A., Carroll, K. & Barratt, J. Long-term phase 2 efficacy of the MASP-2 inhibitor narsoplimab for treatment of severe IgA nephropathy. *ABSTRACT: PO2541, American Society of Nephrology, Kidney week 2021* (2021).

Acknowledgements

Lab technicians Susanne Hansen, Mohamed Ahmed, Gitte Kitlen, Jesper K. Andresen and Camilla Enggaard, Department of Cardiovascular and Renal Research, Institute of Molecular Medicine, University of Southern Denmark, Anette Hansen, Institute of Biomedicine, University of Aarhus and Chloé Sergi, Department of Toxicology and Pharmacology, University of Lausanne are all thanked for skillful technical assistance. Prof. Olivier Staub is thanked for the kind gift of the HEK293 ENaC-expressing cells.

Author contributions

R.Z., S.T., S.H., M.L.H., M.S., K.S., K.M., L.L., E.H., P.S., B.J. designed the study; R.Z., Z.H., P.S. carried out the experiments, R.Z., P.S., B.J. analyzed data; R.Z., S.T., S.H., M.L.H., M.S., K.S., Z.H., K.M. L.L., E.H., P.S., B.J. interpreted results of experiments; R.Z. prepared figures; R.Z., P.S., B.J. drafted the manuscript; R.Z., S.T., S.H., M.L.H., M.S., K.S., Z.H., K.M. L.L., E.H., P.S., B.J. revised the manuscript; R.Z., S.T., S.H., M.L.H., M.S., K.S., Z.H., K.M. L.L., E.H., P.S., B.J. approved the final version.

Funding

The work was supported by grants from the Danish Diabetes Academy funded by the Novo Nordisk Foundation (OL 8201.ID phd0115); Faculty of Health Sciences, University of Southern Denmark; Odense University Hospital (815 (A)); The Beckett Foundation (49091); Bagermester August Jensen and Wife grants (95-102-71226); Grosserer L.F. Foght grants (21.265); Fru Ruth I. E. König-Petersen Research Foundation (71623); Karen Elise Jensen Foundation (ReComiToCKD); the Novo Nordisk Foundation (NNF19OC0058780); The independent Research Fund-Denmark (1030-00330B); Danish Society of Nephrology, travel grants (71406); the Ph.D. school, Faculty of Health Sciences, University of Southern Denmark, travel grants (10-102-00000); Swiss National Science Foundation to EH, 31003A_182478/1.

Competing interests

The authors declare no competing interests.

Additional information

Supplementary Information The online version contains supplementary material available at <https://doi.org/10.1038/s41598-022-20213-8>.

Correspondence and requests for materials should be addressed to R.Z.

Reprints and permissions information is available at www.nature.com/reprints.

Publisher's note Springer Nature remains neutral with regard to jurisdictional claims in published maps and institutional affiliations.



Open Access This article is licensed under a Creative Commons Attribution 4.0 International License, which permits use, sharing, adaptation, distribution and reproduction in any medium or format, as long as you give appropriate credit to the original author(s) and the source, provide a link to the Creative Commons licence, and indicate if changes were made. The images or other third party material in this article are included in the article's Creative Commons licence, unless indicated otherwise in a credit line to the material. If material is not included in the article's Creative Commons licence and your intended use is not permitted by statutory regulation or exceeds the permitted use, you will need to obtain permission directly from the copyright holder. To view a copy of this licence, visit <http://creativecommons.org/licenses/by/4.0/>.

© The Author(s) 2022